Baltic Astronomy, vol. 15, 115–122, 2006.

NEW MODEL ATMOSPHERES FOR HYDROGEN-DEFICIENT STARS: CONTINUOUS AND LINE OPACITIES

N. T. Behara and C. S. Jeffery
Armagh Observatory, College Hill, Armagh BT61 9DG, N. Ireland

Received 2005 August 1

Abstract. The model atmosphere code STERNE has evolved considerably over the years. Most recently, attention has turned to revising the treatment of both continuous and line opacities. Opacity Project photoionization cross-sections have been incorporated and an opacity sampling technique has been implemented. The new opacities and methods are described, while the principal consequences for the models are presented. In studying the application of these new models to atmospheres with extreme chemical compositions, we find the new opacity treatment increases the temperature in the line forming region by 1000–3000 K for extremely hydrogen-poor stars with $T_{\rm eff}$ around 30 000 K. This implies cooler effective temperature measurements for stars of this type.

Key words: stars: atmospheres – stars: chemically peculiar

1. INTRODUCTION

Hydrogen deficiency is a wide spread phenomenon occurring in a variety of stellar objects such as extreme helium stars, hydrogen-deficient binaries, helium-rich subdwarfs, Wolf-Rayet stars, R CrB stars and helium white dwarfs. These hydrogen-deficient systems are believed to evolve by very different processes. R CrB and extreme helium stars evolve by binary merger or last thermal pulse evolution from the white dwarf phase, hydrogen-deficient binary stars through a sequence of mass exchange phases, and helium-rich subdwarfs evolve possibly through white dwarf mergers, late helium flash or common envelope evolution.

Stellar atmosphere models are an essential tool used in the derivation of fundamental stellar parameters, such as effective temperature, surface gravity and overall metallicity, as well as determining individual element abundances. The accuracy of the atmospheric structure obtained from our models is inherently dependent on the quality of the atomic data used and the methods by which they are incorporated into the models, especially in the case of hydrogen-deficient atmospheres.

Because neutral helium is a poor absorber, the effect of continuous and line opacity is of greater importance in hydrogen-deficient stars, shown in Figure 1. The figure on the left shows the emergent flux distribution of hydrogen-rich atmospheres and on the right for hydrogen-deficient atmospheres with ($T_{\rm eff}$, $\log g$) = (10 000, 1.0), (11 000, 1.0), (12 000, 1.0), (13 000, 1.5) and (14 000, 1.5). Continuum-only models are shown by dotted lines and line-blanketed models by

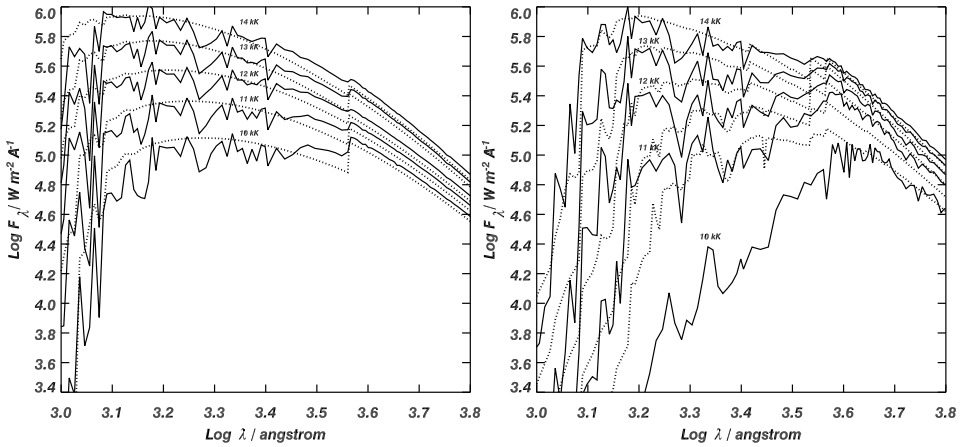

Fig. 1. Importance of line blanketing in hydrogen-rich atmosphere (left panel) and hydrogen-deficient atmospheres (right panel). The figure on the left is from Dudley & Jeffery (1993).

solid lines labeled with effective temperature. The effects of line blanketing on the flux distribution are extremely marked for stars with effective temperatures below 14 000 K.

The entire spectrum of hydrogen-deficient stars comprises an inhomogeneous mix of chemical abundances. For example, in the case of extreme helium stars the hydrogen abundance is roughly 1 part in 10^4, and carbon dominates the opacity at many wavelengths. As a consequence, the carbon abundance greatly influences the atmospheric structure. However, hydrogen-deficient binaries are carbon-poor and nitrogen-rich, while for a few hot R CrB stars $n_{\rm H}$ may be as high as 0.1. In order to model these atmospheres correctly, we should adapt the composition of our models to the composition of stars.

Theoretical work in recent years has provided superior calculations of continuous opacities, and the contribution of absorption lines to the overall opacity has also been an area of progress since STERNE was originally written. We discuss the recent revisions to STERNE and compare some results of the new updated version to the last published version of the code (Jeffery & Heber 1992).

1.1. STERNE – model atmosphere program

The LTE model atmosphere code STERNE was originally developed to study hydrogen-deficient stars. The code is optimized for stars with effective temperatures between 10 000 K and 35 000 K, and extreme compositions dominated by helium, carbon and nitrogen (Schönberner & Wolf 1974; Jeffery & Heber 1992). The model assumes hydrostatic, radiative and local thermodynamic equilibrium, as well as plane-parallel geometry. The radiative transfer equation is solved using Feautrier's scheme, and the temperature correction follows the Unsöld-Lucy procedure.

From 1990 to 2003 the treatment of the continuous opacities followed Kurucz (1979), with the addition of carbon and nitrogen opacities from Peach (1970). The line opacities were calculated using opacity distribution functions (ODF) computed for hydrogen-deficient mixtures from the Kurucz & Peytremann (1975) list of 265 000 lines.

Table 1. Opacity Project photoionization cross-sections used in the continuous opacity calculations.

Element	Ionization stage	Number of states
H	I	55
He	I, II	13, 55
Li	I, II, III	25, 53, 55
Be	I, II, III, IV	55, 25, 54, 55
B	I, II, III, IV	55, 55, 26, 53
C	I, II, III, IV	50, 21, 38, 24
N	I, II, III, IV	36, 50, 32, 39
O	I, II, III, IV	50, 29, 25, 36
F	I, II, III, IV	50, 50, 50, 50
Ne	I, II, III, IV	50, 50, 50, 50
Na	I, II, III, IV	32, 50, 50, 50
Mg	I, II, III, IV	50, 32, 50, 50
Al	I, II, III, IV	41, 50, 31, 50
Si	I, II, III, IV	50, 51, 50, 31
S	I, II, III, IV	50, 50, 50, 50
Ar	I, II, III, IV	50, 50, 50, 50
Ca	I, II, III, IV	50, 17, 50, 50
Fe	III, IV, V, VI	50, 50, 50, 50

2. METHODS

2.1. Continuous opacities

We focus the discussion on the continuous opacities due to bound-free transitions only, as the treatment of free-free absorption and scattering is preserved from the previous version of STERNE.

The Opacity Project (OP, The Opacity Project Team 1995, 1997) data used in the opacity calculations is shown in Table 1. The individual cross-sections must first be resampled on the model wavelength grid before the opacity calculations are carried out, and as a consequence the photoexcitation of the core (PEC) resonances of the cross-sections are not fully resolved. The resampling preserves the cross-sections to within an error of 10%.

The way in which the OP data are included in the model atmosphere code is sufficiently general that any combination of ions may be selected, once the necessary cross-sections have been downloaded from TOPbase (Cunto et al. 1993). Additional cross-sections may be added as they become available.

2.2. Line opacities

We have devised a procedure, loosely based on Sneden et al. (1976) to sample the line opacity directly at each wavelength grid point for all layers in a model atmosphere. Relevant lines are selected from a master list of atomic lines based on the temperature, pressures and abundances of the model at each wavelength and depth point. Approximately 500 000 lines are selected. For each grid point, the

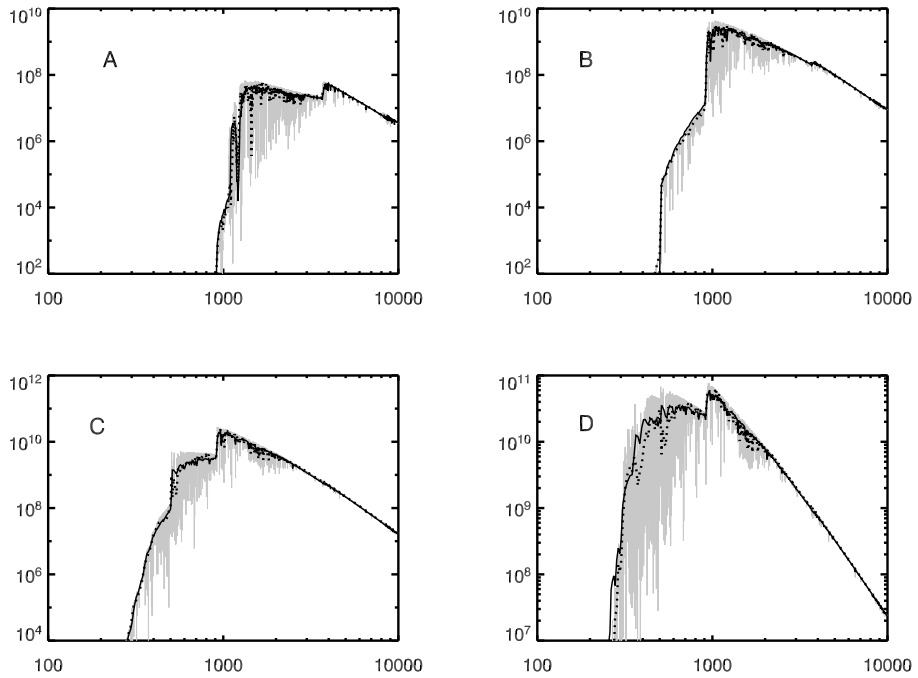

Fig. 2. Solar composition comparisons of the STERNE opacity sampled models to Kurucz's ATLAS9 models. The ATLAS9 models are shown by the black lines. The STERNE models are represented by the grey lines, and also shown resampled on the ATLAS9 grid by the dotted lines. The emergent flux is plotted as a function of wavelength for four $T_{\rm eff}$, log g pairs (see text).

contributions of all selected lines within prescribed search windows are included in the line opacity calculation. The line opacity is calculated using detailed line profiles for each selected spectral line. Computed in this fashion, the opacity sampling (OS) method is able to account for the depth dependence of the variation with wavelength of the line opacities. Lines are selected from the atomic line list compiled by Kurucz & Bell (1995).

2.3. Model verification

A comparison of the STERNE models with Kurucz's ATLAS9 models has been carried out using a solar composition and four effective temperature and gravity pairs. The results are shown in Figure 2.

The emergent flux is plotted as a function of wavelength for A: $T_{\rm eff} = 10\,000$ K, $\log g = 3.0$, B: $T_{\rm eff} = 20\,000$ K, $\log g = 3.0$, C: $T_{\rm eff} = 30\,000$ K, $\log g = 3.5$ and D: $T_{\rm eff} = 40\,000$ K, $\log g = 4.5$. The STERNE model has been resampled on the ATLAS9 grid to allow for comparison. Differences in the models can be accounted for by the different solar abundances used, and differences in the treatment of continuous and line opacities, which alter the model structure. We use the solar abundances of Grevesse & Sauval (1998), while Kurucz uses the abundances by Anders & Grevesse (1989).

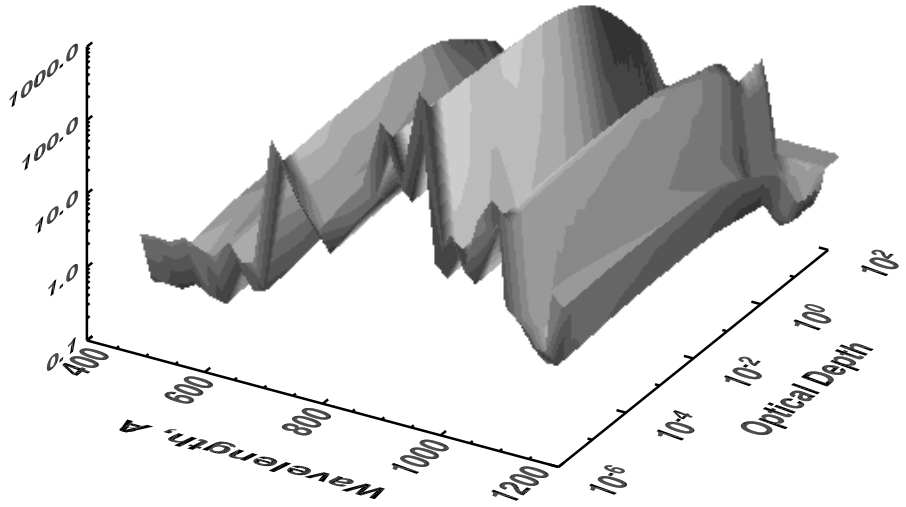

Fig. 3. The ratio of the OP C II continuous opacity to the Peach opacity in a model atmosphere with $T_{\rm eff} = 20\,000$ K and $\log g = 3.0$.

3. RESULTS

We have compared hydrogen-rich and helium-rich models of the opacity sampled version of STERNE with new continuous opacities to the models computed using the ODF version of STERNE. Models have been computed with and without line opacity in order to compare the effect of changing the continuous opacities alone.

Looking at continuum-only models, we find general agreement between the models in the hydrogen-rich case. However, when comparing helium-rich models, we have found that the new opacities produce significant changes in the emergent flux distribution of the atmosphere, particularly in the region 500 Å $< \lambda <$ 1000 Å. The primary cause is the C II continuous opacity.

An increase in the opacity when using the OP cross-sections leads to an increase in the continuum opacity at $\lambda < 1000$ Å, resulting in more UV flux with a steeper continuum at $\lambda > 1200$ Å. A comparison of the C II opacity computed in both models is shown in Figure 3. The ratio of the opacity computed with the OP cross-sections to the opacity computed using the Peach tables (1970) is plotted as a function of optical depth in the atmosphere and as a function of wavelength.

When comparing continuum plus line models, we find that differences in the flux and temperature distributions are far more drastic for the helium-rich case than the hydrogen-rich case.

The plot on the left of Figure 4 shows the effects of the new opacities on the flux distribution of a hydrogen-rich atmosphere and the figure on the right for a helium-rich atmosphere with $T_{\rm eff} = 30\,000$ K and $\log g = 5.0$. The ODF model is shown by the solid line, the OS model by the grey line and the OS model resampled on the ODF wavelength grid by the dotted line. The plots have been cropped to show regions of interest, the integral over the flux remains the same for both models.

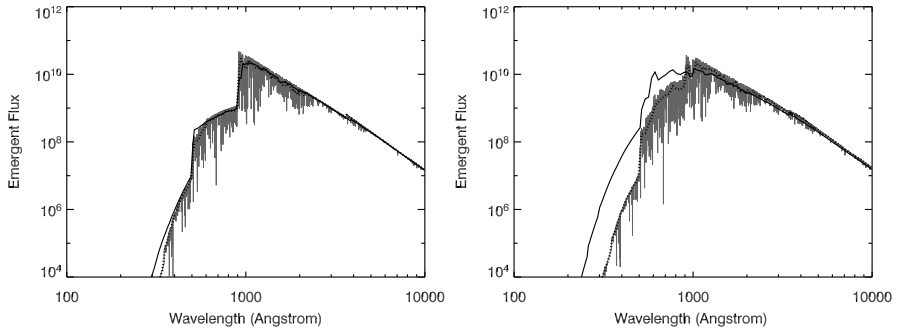

Fig. 4. Flux distributions of hydrogen-rich and helium-rich model atmospheres. The solid line represents the ODF model, and the grey line represents the new OS model, also shown resampled on the ODF grid (dotted line). Model parameters on the left: $T_{\rm eff} = 30\,000$ K, $log\, g = 5.0$, $n_{\rm H} = 0.911$ and $n_{\rm He} = 0.089$. Model parameters on the right: $T_{\rm eff} = 30\,000$ K, $log\, g = 5.0$, $n_{\rm H} = 0.0001$ and $n_{\rm He} = 0.99$, $n_{\rm C} = 0.0099$ and solar metallicity.

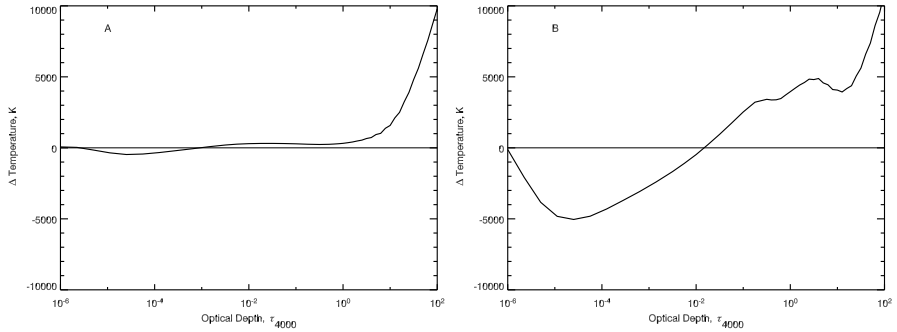

Fig. 5. Differences ($T_{\rm OS} - T_{\rm ODF}$) in the temperature distribution for the models as a function of optical depth. A – hydrogen-rich models from the left plot of Fig. 4, B – helium-rich models from the right plot of Fig. 4.

The effect of the new opacities on the temperature distribution of the atmosphere is shown in Figure 6. The temperature differences ($T_{\rm OS} - T_{\rm ODF}$), are plotted as a function of optical depth for both compositions. The differences in the temperature distribution translate into an approximate increase of up to 3000 K in the line forming region of the atmosphere for a hydrogen-deficient star with $T_{\rm eff} = 30\,000$ K. In the hydrogen-rich case we expect an increase of approximately 300 K.

Figure 6 shows the range of the approximate increase in temperature across the line forming region of both helium-rich and hydrogen-rich high-gravity stars at several effective temperatures. These results show that the new treatment of opacity will have implications in the effective temperature measurements of stars of all compositions and temperatures.

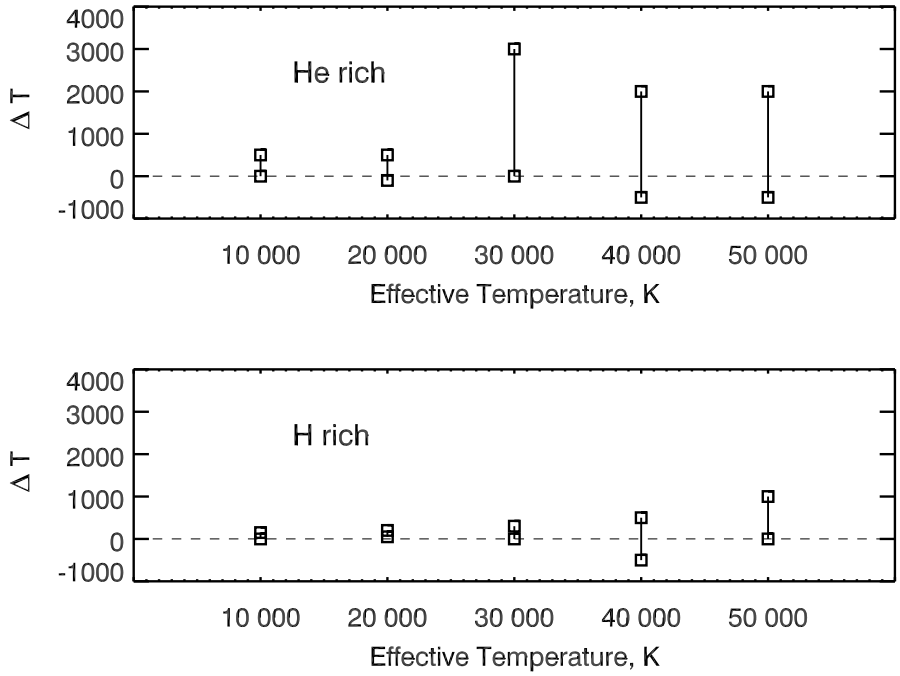

Fig. 6. Differences ($T_{\rm OS} - T_{\rm ODF}$) in the line forming region of the temperature distribution of helium-rich and hydrogen-rich model atmospheres with $(T_{\rm eff}, \log g) =$ $(10\,000, 3.0)$, $(20\,000, 4.0)$, $(30\,000, 5.0)$, $(40\,000, 6.0)$, $(50\,000, 6.0)$. The line forming region has been approximated as the range in optical depth 10^{-2} to 10^{0}.

4. SUMMARY

The treatments of continuous and line opacity in the model atmosphere code STERNE have been revised. Opacity Project cross-sections have been incorporated and an opacity sampling method has been implemented. Results show significant differences for chemically peculiar stars when compared to model atmospheres computed using Kurucz and Peach continuous opacities and an ODF treatment for line opacity. The principal results are that the C II continuous opacity computed using OP cross-sections substantially modifies the flux distribution of hydrogen-deficient atmospheres at $\lambda \sim 1000$ Å, and the new line opacity treatment significantly modifies the temperature distribution of these stars. Effects in the temperature distribution of hydrogen-rich stars of up to 300 K are also seen. These results will have consequences in the effective temperature measurements of stars of all compositions.

Several applications exist for these models. We intend to examine extreme helium stars, helium-rich sdB stars, chemically peculiar subdwarf B stars and hydrogen-deficient binaries.

ACKNOWLEDGMENTS. Research at Armagh Observatory is funded by the Department of Culture, Arts and Leisure, Northern Ireland.

REFERENCES

Anders E., Grevesse N. 1989, Geochim. Cosmochim. Acta, 53, 197

Cunto W., Mendoza C., Ochsenbein F., Zeippen C. J. 1993, A&A, 275, L5

Dudley R. E., Jeffery C. S. 1993, MNRAS, 262, 945

Grevesse N., Sauval A. J. 1998, Space Sci. Rev., 85, 161

Jeffery C. S., Heber U. 1992, A&A, 260, 133

Kurucz R. L. 1979, ApJS, 40, 1

Kurucz R. L., Bell B. 1995, Kurucz CD-ROM 23, Cambridge, SAO

Kurucz R. L., Peytremann E. 1975, SAOSR, 326, 1

Peach G. 1970, MNRAS, 73, 1

Schönberner D., Wolf R. 1974, A&A, 37, 87

Sneden C., Johnson H. R., Krupp B. M. 1976, ApJ, 204, 281

The Opacity Project Team. 1995 in *The Opacity Project*, Vol. 1, Institute of Physics Publishing, Bristol

The Opacity Project Team. 1997 in *The Opacity Project*, Vol. 2, Institute of Physics Publishing, Bristol